The absorption spectrum of 13 CH 4 in the 1.58 μm transparency window (6147–6653 cm –1)

A. Campargue, E. V. Karlovets, E. Starikova, A. Sidorenkoa, Didier Mondelain

The absorption spectrum of $^{13}CH_4$ in the 1.58 µm transparency window (6147-6653 cm^{-1})

A. Campargue [a*], E. V. Karlovets [b,c], E. Starikova [b, d], A. Sidorenko [a], D. Mondelain [a]

[a] *Univ. Grenoble Alpes, CNRS, LIPhy, 38000 Grenoble, France*
[b] *Tomsk State University, Laboratory of Quantum Mechanics of Molecules and Radiative Processes, 36, Lenin Avenue, 634050, Tomsk, Russia*
[c] *Harvard-Smithsonian Center for Astrophysics, Atomic and Molecular Physics Division, Cambridge, MA, USA;*
[d] *Laboratory of Theoretical Spectroscopy of IAO SB RAN, av. 1, Akademician Zuev square, 634021 Tomsk, Russia*

Number of Figures: 9

Number of Tables: 2

Running Head: *$^{13}CH_4$ absorption near 1.58 µm*

Keywords: *methane; $^{13}CH_4$; absorption spectroscopy; HITRAN; Empirical lower state energy*

*Corresponding author: Alain.Campargue@univ-grenoble-alpes.fr

Abstract

The room temperature absorption spectrum of $^{13}CH_4$ is recorded by high sensitivity cavity ring down spectroscopy (CRDS) near 1.58 µm. The investigated region (6147-6653 cm^{-1}) corresponds to a spectral region of weak absorption located between the strong bands of the tetradecad and icosad. The sensitivity of the recordings allowed for the measurement of more than 13000 lines for which line centers and line intensities are derived using a multiline fitting program. The obtained list is the first extensive list of ^{13}C enriched methane in the region. It is believed to include a significant number of lines of $^{13}CH_3D$.

In addition, 185 lines were measured at 80 K by direct absorption spectroscopy (DAS) near 6600 cm^{-1}. The line intensity detectivity threshold is on the order of a few 10^{-29} cm/molecule for the CRDS recordings at 296 K and 10^{-26} cm/molecule for the DAS recordings at 80 K. From the intensity ratio of the lines in common in the 296 K and 80 K empirical line lists near 6600 cm^{-1}, 438 empirical values of the lower state energy level (E_{emp}) were derived. An additional set of 200 E_{emp} values were obtained by combining the present CRDS line intensities to DAS literature data near 6150 cm^{-1}.

The comparison to the TheoReTS *ab initio* line list shows an overall very good agreement on the line intensity. Significant deviations on the order of 0.1 cm^{-1} are noted for line positions. The obtained experimental data will be valuable to tune *ab initio* line positions to empirical values in future versions of the theoretical line lists.

Finally, a first set of 900 lines belonging to the $5\nu_4$ and $\nu_2+4\nu_4$ bands of the icosad are rovibrationally assigned on the basis of an effective Hamiltonian model. The energy values of the involved vibrational sublevels are determined.

1. INTRODUCTION

The present work aims at extending the knowledge of the absorption spectrum of the $^{13}CH_4$ minor isotopologue of methane in a spectral region of weak absorption (or transparency window) of importance for planetary applications, in particular for Titan. As a rule, the general appearance of the absorption spectra of $^{12}CH_4$ and $^{13}CH_4$ is very similar because the isotopic substitution of the central carbon atom leads to global shifts of the different variational bands limited to a few tens wavenumbers in the near infrared. (This not the case for CH_3D - see below)

The 1.58 µm window is located between strong bands of the tetradecad and of the icosad at low and high energies, respectively (see **Fig. 1**). The tetradecad (14 vibrational levels and 60 sub-levels) and the icosad (20 vibrational levels and 134 sub-levels) are polyads of vibrational levels in strong rovibrational interaction. The number of levels involved and the strength of the interactions lead to a highly congested spectrum with no apparent regular structure except for the strong $2\nu_3$ and the $\nu_2+2\nu_3$ bands at 6000 and 7500 cm^{-1}, respectively.

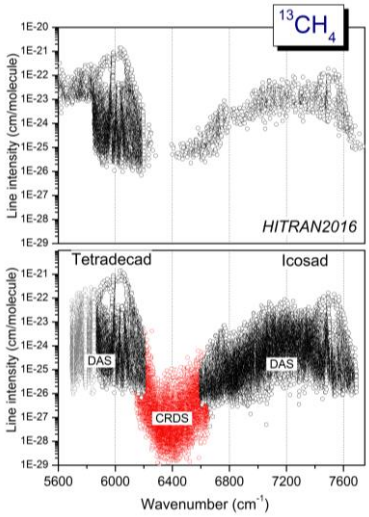

Fig. 1
Overview of the $^{13}CH_4$ line list between 5600 and 7700 cm^{-1}.
Upper panel: Line list provided by the HITRAN2016 database (line intensities correspond to the pure $^{13}CH_4$ species)
Lower panel: Empirical line lists obtained by direct absorption spectroscopy (DAS) in the tetradecad and icosad and by CRDS in the present work (red and black, respectively).

Direct absorption laser spectroscopy (DAS) and Fourier transform spectroscopy (FTS) do not provide sufficient sensitivity to characterize the 1.58 µm window of methane. The only previous study in the region was performed by cavity ring down spectroscopy (CRDS) with a sample with natural isotopic abundance. Recordings performed at room temperature and with a CRDS cell cooled at liquid nitrogen temperature allowed for the elaboration of two empirical line lists for methane in natural

isotopic abundance, at 296 K and 80 K. The corresponding empirical values of the lower state energy level, E_{emp}, were determined using the two-temperature method (see below). Being located at the low energy edge of the icosad and thus less affected by interactions, the $^{12}CH_4$ lines of the $5\nu_4$, $\nu_2+4\nu_4$, $\nu_1+3\nu_4$ bands could be rovibrationnally assigned at 80 K. Their line positions could be modelled by an effective Hamiltonian obtained by reduction of the full Hamiltonian of methane nuclear motion based on an *ab initio* potential energy surface.

The assignment of the $^{12}CH_4$ room temperature spectrum has not been reported so far. In its present version, the HITRAN database reproduces the CRDS line list at 296 K as part of the WKLMC line list and includes a limited number of rovibrational assignments (from Ref. []). It is worth mentioning that, in spite of its low isotopic relative abundance (about 5×10^{-4}), CH_3D has a large relative contribution to the absorption in the 1.58 µm methane transparency window. As a consequence of the strong isotopic shift of the CD stretching frequency (ν_2) compared to CH, the $3\nu_2$ band near 6430 cm^{-1} falls in the region of weakest CH_4 absorption. As a result, CH_3D in natural abundance (about 5×10^{-4}) represents between 10 and 20% of the methane absorption at 296 K in the 6300-6500 cm^{-1} interval [papier CH3D]. At low temperature (80K), this percentage increases up to 75 % near 6300 cm^{-1}. Due to the importance of the 1.58 µm window for planetary application (the D/H isotopic ratio is strongly dependent on the considered planet), a spectroscopic study was devoted to CH_3D in the region. The spectrum of high purity CH_3D was recorded both at room temperature and at 81 K. As CH_3D transitions in the region are strong (line intensities up to 10^{-22} cm/molecule), the DAS technique provided sufficient sensitivity ($\alpha_{min} \approx 5\times10^{-8}$ cm^{-1}). On the basis of this work, the lines of CH_3D present in the spectrum of "natural" methane could be systematically identified in the 1.58 µm window.

A similar work remains to be done for the $^{13}CH_4$ species. As illustrated in **Fig.1,** only the strongest $^{13}CH_4$ lines (intensity larger than about 4×10^{-26} cm/molecule for pure $^{13}CH_4$) were detected and could be identified in the spectrum of "natural" methane. The DAS technique applied to $^{13}CH_4$ in the tetradecad below 6200 cm^{-1} and in the icosad above 6600 cm^{-1} does not provide sufficient sensitivity in the 1.58 µm window. In the present work, we report the first high sensitivity study of the $^{13}CH_4$ spectrum in the region. The spectra of methane highly enriched in ^{13}C were recorded by CRDS at room temperature. The CRDS recordings and the line list construction are detailed in the next paragraph. In the discussion (Section 4), we present a comparison to *ab initio* calculations and to the $^{13}CH_4$ HITRAN list in the region.

2. EXPERIMENT AND CONSTRUCTION OF THE LINE LIST

The CRDS spectrum of $^{13}CH_4$ at room temperature was recorded from 6147 to 6653 cm^{-1} with a fibered CRDS spectrometer using distributed feed-back (DFB) diode lasers as light sources. The stainless steel high finesse cell (HFC) (l= 1.42 m, Φ_{in}= 11.7 mm) is fitted by a pair of super mirrors (~99.998% reflectivity) giving rise to ring down times on the order of 200 μs. The whole spectral region was continuously covered with the help of twenty-four fibered DFB lasers. The DFB lasers driven at a constant current of 140 mA have a tuning range of about 40 cm^{-1} for a temperature scan from -10 to 60°C. About 40 ring down events were averaged for each spectral data point separated by approximately 2×10^{-3} cm^{-1}. A complete DFB temperature scan was achieved within 65 minutes. Ring down (RD) events were obtained by switching off the laser beam with the acousto-optic modulator (AOM) used on its order +1, each time a longitudinal mode of the HFC falls in coincidence with the laser frequency. Resonances were achieved by modulating the HFC length over one free spectral range thanks to a piezo tube supporting the output mirror [Romanini1997]. Ring down times, τ, were measured by fitting with a purely decreasing exponential function the signal measured with an InGaAs photodiode. The obtained loss rate, $1/c\tau$, is the sum of the loss rate with the cell evacuated, $1/c\tau_0$, and of the extinction coefficient, $\alpha(\nu)$, due to the gas:

$$\frac{1}{c\tau(\nu)} = \frac{1}{c\tau_0(\nu)} + \alpha(\nu) \qquad (1)$$

where c is the speed of light.

The CRDS cell was filled with pure $^{13}CH_4$ (ISOTEC ^{13}C enrichment > 99%). Series of recordings were performed for two pressure values. A pressure of 7.5 Torr was adopted in the center and high energy range of the window (6254-6653 cm^{-1}) while recordings were performed at 1.0 Torr in the low and high frequency edges (6147-6283 cm^{-1}) and 6520- 6653 cm^{-1}). The pressure value given by a capacitance gauge (Baratron) was continuously monitored during the recordings as well as the cell temperature (296±1 K).

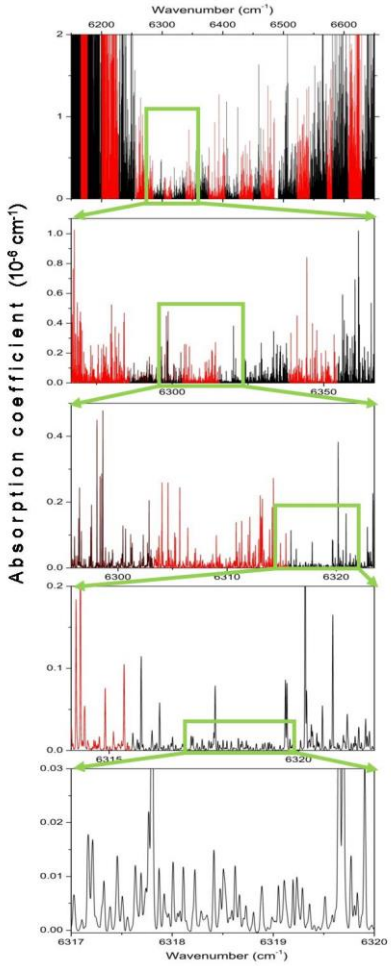

Fig. 2
Overview of the $^{13}CH_4$ CRDS recordings between 6150 and 6650 cm^{-1}. The successive enlargements reveal the high spectral congestion of the spectrum. The sample pressure was 7.5 Torr. The alternate colors correspond to recordings performed with different distributed feed-back diode lasers

The line list construction was particularly laborious. First, as illustrated in **Fig. 2**, the spectral congestion is considerable. The CRDS sensitivity allows for the detection of very weak lines down to a detectivity threshold on the order of 10^{-29} cm/molecule while the strongest lines have intensity four orders of magnitude larger. As a result, the density of detected transitions is high, on the order of 25 lines/ cm^{-1}. The line centers and line intensities were obtained by using a homemade interactive least squares multi-lines fitting written in LabVIEW. The line parameter derivation consisted in delimitating narrow spectral intervals corresponding to groups of (overlapping) lines which could be fitted independently. For each interval, line centers, integrated absorption coefficients, the Lorentzian

contribution of each line and a baseline (assumed to be a linear function of the wavenumber) were provided by the fitting procedure. The line intensity, S_{ν_0} (cm/molecule), of a rovibrational transition centered at ν_0, was obtained from the integrated absorption coefficient, A_{ν_0} (cm^{-2}/molecule):

$$A_{\nu_0}(T) = \int_{line} \alpha_\nu d\nu = S_{\nu_0}(T)\, N \tag{2}$$

where ν is the wavenumber in cm^{-1}, α_ν is the absorption coefficient in cm^{-1} obtained from the cavity ring down time (Eq. 2) and N is the molecular concentration in molecule/cm^3 obtained from the measured pressure and temperature values: $P = NkT$. The agreement between the spectral simulation and the CRDS spectrum is illustrated in **Fig. 3**.

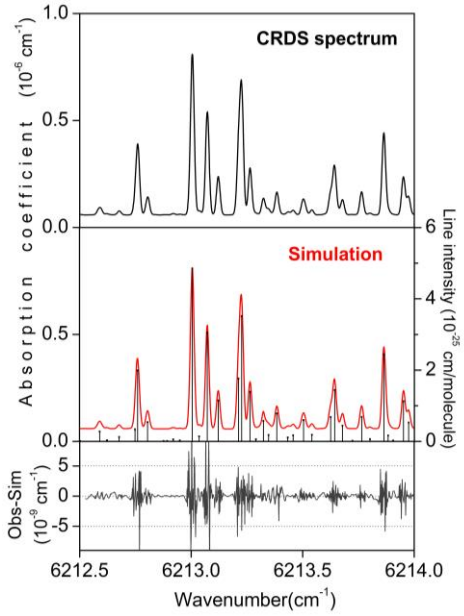

Fig. 3. Line parameter retrieval
Upper panel: CRDS spectrum of $^{13}CH_4$ near 6213 cm^{-1} (P= 1.0 Torr, T= 297 K)
Medium panel: fitted spectrum using a Voigt profile for each line and corresponding stick spectrum,
Lower panel: Residuals between the simulated and experimental spectra.

Each 40 cm^{-1} wide spectrum corresponding to one DFB recording was calibrated independently on the basis of the wavenumber values provided by a Fizeau type wavemeter (WSU-30 Highfinesse, 5 MHz resolution and 20 MHz accuracy). The calibration was refined using reference line positions of H_2O (present as an impurity) from the HITRAN database [Gordon2017]. We estimate the uncertainty on the position of well isolated lines to be 1×10^{-3} cm^{-1}.

Additional difficulties were due to the fact that the absorption of some lines were too strong for CRDS, making the light intensity transmitted by the cell insufficient for accurate measurement of the

RD times. This issue concerns lines on the low and high energy edges of the studied interval. In the 6147-6200 cm^{-1} interval which includes lines with intensity as large as 10^{-23} cm/molecule, line parameters obtained by DAS in Ref. were adopted for the strong lines. At high energy (6520-6653 cm^{-1}) recordings at 1 Torr and 7.5 Torr are both available. Weaker lines are detected at 7.5 Torr but the strongest lines cannot be measured at that pressure. In that frequency interval, for each DFB laser diode, the line list was obtained by incorporating the 1 Torr line parameters of the strong lines in the 7.5 Torr line list.

Then, impurity lines were systematically searched and removed from all the line lists. A significant number of water lines were detected above 6400 cm^{-1}. The presence of water is believed to be due to desorption from the cell. Water relative concentration was evaluated to be no more than 2×10^{-3}. Lines of CO_2 and very weak lines of acetylene were also identified with corresponding relative concentration less than 10^{-4} and 5×10^{-7}. Finally, we checked that our lists do not include lines of the $^{12}CH_4$ major isotopologue, confirming the high isotopic purity of the used $^{13}CH_4$ sample.

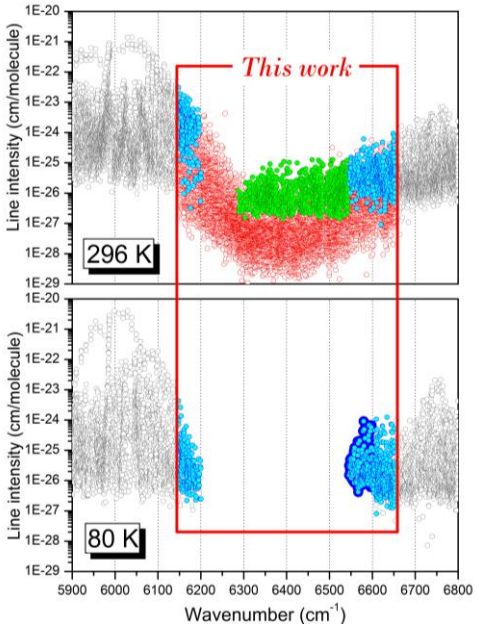

Fig. 4
Overview of the $^{13}CH_4$ line list in the 1.58 µm transparency window.
Upper panel: Lists at 296 K obtained in this work by CRDS (red), in Ref. [] and Ref. [] for the tetradecad and icosad regions (grey circles). Lines with full rovibrational assignment are highlighted in green.
Lower panel: Lists at 80 K obtained in this work by DAS between 6545 and 6600 cm^{-1} (blue circles), in Ref. [] and Ref. [] for the tetradecad and icosad regions (grey circles).
On the two panels, lines with lower state energy value derived by combining the present CRDS data at 296 K and the DAS data at 80 K are highlighted with light blue.

The complete line list provided as Supplementary Material was obtained by gathering the line lists corresponding to the different DFB laser diodes. It includes a total of 13032 lines with intensity at 296 K ranging between about 10^{-29} and 1.8×10^{-23} cm/molecule.

3. ANALYSIS AND DISCUSSION

3.a. Empirical determination of the lower state energy

The two temperature-method uses the temperature dependence of the line intensity to derive the empirical value of the lower state energy of the considered transition. The *2T*-method was successfully applied to DAS spectra of $^{13}CH_4$ recorded at 296 K and 80 K in the tetradecad (up to 6200 cm^{-1}) and in the icosad (from 6600 cm^{-1}). In the present work, CRDS recordings were not performed at low temperature but the DAS recordings in the icosad were extended down to 6543 cm^{-1}. The spectra were recorded at a pressure of 6.0 Torr with an absorption pathlength of 282 cm. The reader is referred to Ref. [] for the description of the DAS spectrometer and cell cooled at liquid nitrogen temperature. Three DFB diodes were used to cover the 6545-6602 cm^{-1} interval. The comparison of the DAS spectrum at 80 K to the CRDS spectrum at room temperature presented in **Fig. 5** illustrates the drastic change of the appearance of the spectrum by cooling. Depending on the lower state energy of the considered transitions, lines exhibit very different temperature dependence.

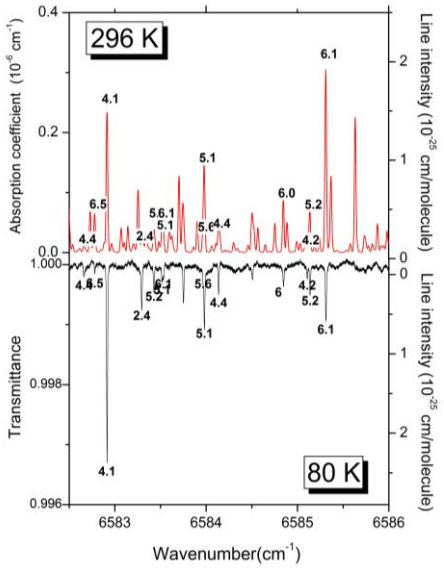

Fig. 5.
Example of empirical lower state J_{emp} values derived for $^{13}CH_4$ transitions near 6584 cm^{-1}.
Upper panel: CRDS spectrum at 297 K (*P*= 1.0 Torr)
Lowerpanel: DAS spectrum at 80 K (*P*= 6.0 Torr)
Empirical J_{emp} values derived by the 2*T*-method are indicated for the coinciding lines. Note the difference of sensitivity of the CRDS and DAS recordings.

A set of about 200 lines were measured and gathered with the 80 K DAS list of Ref. . As a result, *2T*-method could be applied in the 6147-6200 cm^{-1} and 6547-6653 cm^{-1} intervals which are in common between the DAS lists at 80 K and the present CRDS list at room temperature (see **Fig. 4**).

The lower state energy (E_{emp}) of the transitions in common in the two datasets was determined from the ratio of line intensities measured at 80 and 296 K ([7,15]:

$$\frac{S_{v_0}(T_1)}{S_{v_0}(T_0)} = \frac{Z(T_0)}{Z(T_1)} \exp\left[- E_{emp} \left(\frac{1}{kT_1} - \frac{1}{kT_0} \right) \right], \qquad (3)$$

where S_{v_0} and Z are the intensity and partition function, respectively (T_0 = 296 K, T_1= 80 K).. The $^{13}CH_4$ partition function for the corresponding temperatures was taken from HITRAN [6]: $\frac{Z(297\,K)}{Z(80\,K)} = 7.09016$. Lines corresponding to the same transition at 296 K and 80 K were associated automatically when their line centers position coincidence criterion fixed to within 0.003 cm^{-1}. This value is about third of the Doppler full width of the $^{13}CH_4$ line at 80 K and corresponds to the estimated combined error bars of the line center determinations. This position criterion allowed us deriving the E_{emp} values of 200 and 438 lines in the 6147-6200 cm^{-1} and 6547-6653 cm^{-1} interval, respectively. The associated lines are highlighted with light blue on **Fig. 4**. As the sensitivity of the DAS recordings is significantly lower than that of the CRDS recordings, E_{emp} values were determined for most of the transitions of the 80 K dataset (about 80%).

The lower state rotational quantum number, J_{emp}, was obtained using the rigid approximation, $E_{emp} \approx B_0 J(J+1)$ where B_0= 5.214 cm^{-1} is the $^{13}CH_4$ principal rotational constant. The lower state empirical J_{emp} values were computed from $J_{emp} = \sqrt{\frac{1}{4} + \frac{E_{emp}}{B_0}} - \frac{1}{2}$. As an example, the derived empirical *J* values have been indicated on the piece of the spectra displayed in **Fig. 5**. In the displayed interval, the obtained J_{emp} values show a clear propensity to be close to integers. However, the insufficient sensitivity of the DAS recordings limits the accuracy of the intensity values at 80K and a significant number of J_{emp} values are not integer.

The above derivation of J_{emp}, assumes that the measured lines belong to $^{13}CH_4$ and not to $^{13}CH_3D$ while we mentioned in the introduction that $^{13}CH_3D$ is expected to contribute to the spectrum in the region. As illustrated in Fig. 6 of Ref. [], the strongest bands of $^{13}CH_3D$ are not located in the two intervals where we apply the 2*T*-method but in the center of the window. For instance, taking into account an estimated isotopic shift of 20 cm^{-1}, compared to $^{12}CH_3D$, the $3\nu_2$ band of $^{13}CH_3D$ is predicted to be centred near 6410 cm^{-1}

The list at 80 K in the 6147-6200 and 6547-6653 cm^{-1} intervals is provided as Supplementary Material and includes the position and intensity of the coincident lines at 296 K used to derive the E_{emp} and J_{emp} values. Similarly, in the 296 K list, we provide the position and intensity of the coincident lines at 80 K. A sample of the 80 K list is reproduced in **Table 1**

Table 1
Wavenumbers and intensities of $^{13}CH_4$ absorption lines recorded by DAS at 80 K and CRDS at 296 K near 6610 cm^{-1}. The empirical values of the lower state energy, E_{emp} and corresponding J_{emp} values were obtained by the 2*T*-method for the transitions whose centers at 296 K and 80 K coincide within 0.003 cm^{-1}. This Table is a section of the list attached as Supplementary Material. A similar list is also provided for *T*= 296 K.

T= 80 K		*T*= 296 K			
Line center (cm^{-1})	*Line intensity (cm/molecule)*	*Line center* (cm^{-1})	*Line intensity (cm/molecule)*	E_{emp} (cm^{-1})	J_{emp}
6609.2058	2.6120E-25	6609.2082	5.4290E-26	29.15	1.91
6609.2237	8.2893E-26	6609.2230	4.8980E-26	108.76	4.08
6609.3758	2.3495E-27	6609.3784	2.9630E-26	341.97	7.59
6609.4130	3.0663E-26	6609.4129	2.5740E-26	135.51	4.61
6609.4331	8.0771E-28	6609.4340	6.0580E-26	477.83	9.06
6609.4687	2.0641E-25	6609.4694	1.4610E-25	122.52	4.36
6610.2387	4.6773E-26	6610.2385	7.4320E-26	184.13	5.45
6610.2976	2.9926E-26	6610.2947	3.1380E-26	152.46	4.92
6610.3406	1.3647E-25	6610.3400	1.0440E-25	128.44	4.48
6610.3785	2.9144E-27	6610.3768	4.7970E-27	186.82	5.49
6610.4732	4.3376E-27	6610.4722	2.9990E-26	296.18	7.03
6610.4857	8.2626E-27	6610.4855	1.5790E-26	198.20	5.67
6610.8015	4.8685E-25	6610.8020	1.6590E-25	66.82	3.11
6611.0616	7.6023E-26	6611.0624	1.1840E-25	182.61	5.42
6611.0756	1.4795E-26	6611.0768	3.7700E-26	220.12	6.00
6611.4624	1.5330E-26				
6611.4725	5.6125E-27				
6611.4977	3.0826E-27	6611.4956	1.4590E-25	442.75	8.71
6611.7867	5.3253E-27	6611.7877	1.7390E-26	239.02	6.27

3.b. Comparison to the HITRAN and TheoReTs databases

The overview included in **Fig. 1** shows that the HITRAN2016 list of $^{13}CH_4$ is largely incomplete in the 1.58 µm transparency window and in the icosad. Indeed, while in the $2\nu_3$ region of the tetradecad around 6000 cm^{-1}, HITRAN list reproduces the results of a DAS study of pure $^{13}CH_4$, in the region above 6200 cm^{-1}, the $^{13}CH_4$ line parameters of the HITRAN list were obtained from studies of natural methane. The natural relative abundance of $^{13}CH_4$ being about 1.1 % many $^{13}CH_4$ lines were obscured by stronger $^{12}CH_4$ lines or poorly measured. The present measurements in the transparency window together with the recent DAS study of pure $^{13}CH_4$ in the icosad will be valuable to complete the HITRAN.

The TheoReTS *ab initio* line list computed by the Reims-Tomsk collaboration [12,14,15] is accessible *via* the TheoReTS information system [10] (http://theorets.univ-reims.fr, http://theorets.tsu.ru). The TheoReTS list was computed by variational method [11,46,47] using recent *ab initio* potential and dipole moment surfaces [31,48,49] conducting to RNT (Rey-Nikitin-Tyuterev) line lists as described in [12,42]. This is illustrated on **Fig. 6**: while the overview comparison of the CRDS spectra with the TheoReTS list at room temperature shows an excellent agreement. The enlargement around 6433 cm^{-1} shows a good coincidence between the experimental and *ab initio* intensities but some *ab initio* line positions show deviations on the order of 0.1 cm^{-1} or more. The

present measurement will allow for a tuning of the calculated line positions according to experimental or empirical values.

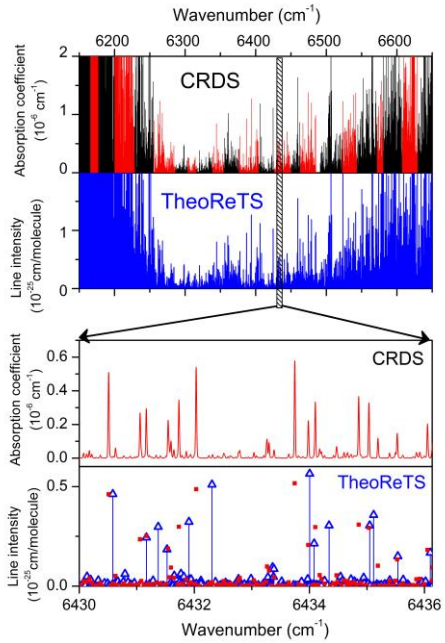

Fig. 6.
Comparison of the CRDS spectrum of $^{13}CH_4$ (*P*= 7.5 Torr) with the *ab initio* TheoReTS line list at 296 K.
Upper panels: Overview between 6150 and 6650 cm^{-1}. The alternate colors correspond to recordings performed with different distributed feed-back diode lasers
Lower panels: Enlargement around 6433 cm^{-1} showing the good agreement for the line intensities and significant deviations of the line positions TheoReTS list (blue sticks). On the lowest panel, the red symbols correspond to the CRDS line list.

~~**Table 2**~~
~~Statistics for the empirical line lists of $^{13}CH_4$ in the 5695.3-5850.4 cm^{-1} region.~~

	~~Sum of intensities (cm/molecule)~~	~~Number of lines~~	~~Number of E_{emp}~~
~~This work~~	~~1.068×10^{-21}~~	~~13030~~	~~900 assignments /638 E_{emp} values~~
~~TheoReTS [12]~~	~~1.076×10^{-21}~~	~~35427~~	

The intensity cut off of the TheoReTS lists is fixed to 1×10^{-29} cm/molecule. Experimentally, this detection limit was achieved only in the most transparent region around 6400 cm^{-1} (see **Fig. 1**) and thus a considerable number of very weak calculated $^{13}CH_4$ lines are missing in our list. The sum of the

intensities measured by CRDS between 6147 and 6653 cm^{-1} is 1.068×10^{-21} cm/molecule while the sum of the *ab initio* intensities in the same spectral interval is 1.076×10^{-21} cm/molecule. Such a good agreement within the experimental uncertainty on the intensity measurements might be fortuitous but it indicates that the missing lines have a very small contribution.

3.c. Rovibrational assignments

The TheoReTS line list does not provide full rovibrational assignment but only the J value, symmetry, ??? please complete Eugenia. In the 296K line list provided as Supplementary Material, we give a first set of 900 rovibrational assignments in the center of the window between 6284 and 6543 cm^{-1}. The assigned lines are highlighted on **Fig. 4**. The assignments were limited to cold band transitions of the icosad with line intensities larger than 2×10^{-27} cm/molecule. They were obtained on the basis of the effective Hamiltonian (EH) model obtained in our previous analyses of cold spectra of $^{13}CH_4$ methane [1-3]. The initial non-empirical EH for the methane polyads was constricted? from the potential energy surface (PES) [4] and dipole moment surfaces (DMS) [5] *via* high order Contact Transformation (CT) procedure [6,7]. Then some diagonal EH and resonance coupling parameters were empirically optimized as the assignment and experimental data treatment progressed. Finally, the EH model describes 7077 observed and assigned lines transitions of the $^{13}CH_4$ tetradecad with *rms* deviation of 1.35×10^{-3} cm^{-1}. Using this model a list of predicted ro-vibrational transitions for the range under investigation was created allowing us to assign 901 lines of the $5\nu_4$ and $\nu_2+4\nu_4$ bands of the icosad. The statistics of the assigned transitions is presented in **Table 2** together with the predicted (quel genre de predictions?? Qd tu as P1, c'est une valeur experimentale??) values for band centers. In the future, the assignments will be extended to the entire icosad for which a large set of E_{emp} values has been derived by the *2T*-method []. Eugenya qqs phrases d'ouverture pour les attributions??

Table 2:
Overview of the rovibrational assignments of the $^{13}CH_4$ spectrum at 296 K between 6284 and 6543 cm^{-1}.

Band	Sublevel	Band centre * (cm^{-1})	Positions	
			Nb.	J_{min}, J_{max}
$5\nu_4$	F_2 1[a]	6342.372	58	1-8
	A_1	6370.408	43	2-8
	F_1 1[b]	6393.259	100	1-8
	F_2 2[a]	6413.726	164	0-8
	E	6470.409	54	1-8
	F_2 3[a]	6470.611	88	0-8
	F_1 2[b]	6492.112	56	2-8
	F_2 4[a]	6501.303	101	1-8
$\nu_2+4\nu_4$	E 1[c]	6589.064	33	4-8
	F_1 1[d]	6609.599	66	3-8
	A_1 1[e]	6626.582	1	8-8
	F_2 1[f]	6628.235	22	6-8
	E 2[c]	6651.817	4	4-8
	A_2 1[g]	6653.391	3	8-8
	F_2 2[f]	6687.808	36	5-8

	F_1 2[d]	6692.019	10	5-8
	E 3[c]	6698.724	4	6-8
	F_2 3[f]	6702.476	16	6-8
	A_1 2[e]	6707.815	5	6-8
	A_2 2[g]	6715.917	2	7-8
	F_1 3[d]	6724.873	7	7-8
	E 4[c]	6735.632	28	3-8
Total			**901**	

Notes

* predicted band centers

The vibrational sublevels are enumerated here for each band for a given symmetry type. The ranking numbers within the Tetradecad are the following:

[g] *N*= 1, *N*= 2, *N*= 3, and N= 4 for F_2 1, F_2 2, F_2 3, F_2 4;

[b] *N*= 1 and *N*=2 for F_1 1 and F_1 2;

[c] *N*=2, *N*=3, *N*= 4 and *N*=5 for E 1, E 2, E 3 and E 4;

[d] *N*= 3, *N*=4, and *N*= 5 for F_1 1, F_1 2 and F_1 3;

[e] *N*= 2 and *N*= 3 for A_1 1 and A_1 2;

[f] *N*= 5, N= 6 and *N*= 7 for F_2 1, F_2 2 and F_2 3;

[g] *N*= 1 and *N* =2 for A_2 1 and A_2 2.

Commenté [AC1]: Je comprends pas, cc'est evident?

4. CONCLUDING REMARKS

975 lines in hitran

In this work, empirical line lists for $^{13}CH_4$ at 80 K and 296 K have been elaborated in the very congested center of the tetradecad (5695.32-5850.49 cm^{-1} excluding the 5718.82-5724.25 and 5792.75-5812.11 cm^{-1} intervals). The constructed lists include 3300 and 2070 lines at room temperature and liquid nitrogen temperature, respectively, allowing for the derivation of 1530 empirical values of the lower state energy level using the 2*T*-method. These results will be used together with the results of a similar study performed recently with natural methane in the same region [9], to extend to lower energy the WKLMC list covering the 5852–7919 cm^{-1} range [17,23]. Note that the present DAS recordings were used in Ref. [9] to identify the $^{13}CH_4$ lines present in the DAS spectra of natural methane (1.1 % relative concentration abundance).

The obtained experimental data will be valuable for extending theoretical studies of the isotopic effects [24] in highly excited vibrational states of methane. In Ref. [9], an important part of the $^{12}CH_4$ lines in the region were rovibrationnally assigned using an effective Hamiltonian model developed in Refs. [20-22]. The assignment of the experimental $^{13}CH_4$ lines reported in the present paper will benefit from *ab initio* predictions of the $^{12}C \rightarrow ^{13}C$ isotopic shifts in vibrational band centers. These shifts (up to a few tens cm^{-1}, depending on the excited vibrational state) are predicted with an accuracy much higher than that of the absolute value of the band centers [24]. As they are mostly constant for a given vibrational band, the calculated isotopic shifts allow finding one-to-one correspondence between $^{12}CH_4$ and $^{13}CH_4$ lines. Thus, the next step of the present project will be to transfer the $^{12}CH_4$ assignments of Ref. [9] to the present $^{13}CH_4$ line lists on the basis of the predicted values of the vibrational isotopic shifts. The agreement between the obtained assignments and the E_{emp} values presently obtained will be used as validation tests.

The $^{13}CH_4$ HITRAN2016 line list in the region has GOSAT2009 origin [3] and consists of less than 400 lines from which only about 50 have associated lower state energy values (the rest are left with a 333.33 cm^{-1} default value). About one third of the HITRAN2016 assignments are found in contradiction with the observed temperature dependence of the intensity of the corresponding line. The comparison of the DAS spectra of $^{13}CH_4$ to the TheoReTS *ab initio* line list [12] indicates that the line lists constructed in this work will be valuable to adjust the *ab initio* positions to their empirical counterparts.

Acknowledgments

This work was performed in the frame of the ANR project e_PYTHEAS (ANR-16-CE31-0005).

References:

1. Starikova E, Nikitin AV, Rey M, Tashkun SA, Mondelain D, Kassi S, Campargue A, Tyuterev VlG. Assignment and modeling of the absorption spectrum of $^{13}CH_4$ at 80 K in the region of the $2\nu_3$ band (5853–6201 cm^{-1}). J Quant Spectrosc Radiat Transf 2016;177:170–80.
2. Starikova E, Sung K, Nikitin A, Rey M, Mantz AW, Smith MAH, The $^{13}CH_4$ absorption spectrum at 80 K: Assignment and modeling of the lower part of the Tetradecad in the 4970–5470 cm^{-1} spectral range. J Quant Spectrosc Radiat Transfer 2018;206:306–12.
3. Starikova E, Sung K, Nikitin A, Rey M, Assignment and modeling of the $^{13}CH_4$ cold absorption spectrum in the 5471–5852 cm^{-1} spectral range. J Quant Spectrosc Radiat Transfer 2019, *in preparation*.
4. Nikitin AV, Rey M, Tyuterev VlG. Rotational and vibrational energy levels of methane calculated from a new potential energy surface. Chem Phys Lett 2011;501:179–86.
5. Nikitin AV, Rey M, Tyuterev VG. New dipole moment surfaces of methane. Chem Phys Lett 2013;565:5–11.
6. Tyuterev VlG, Perevalov VI. Generalized contact transformations for quasi-degenerate levels. Chem Phys Lett 1980;74:494–502.
7. Tyuterev Vl G, Tashkun SA, Rey M, Kochanov RV, Nikitin AV, Delahaye T. Accurate spectroscopic models for methane polyads derived from a potential energy surface using high-order contact transformations. J Phys Chem A 2013;117:13779–805.

References

1. L.R. Brown, K. Sung, D.C. Benner, V.M. Devi, V. Boudon, T. Gabard, C. Wenger, A. Campargue, O. Leshchishina, S. Kassi, D. Mondelain, L. Wang, L. Daumont, L. Régalia, M. Rey, X. Thomas, V.G. Tyuterev, O.M. Lyulin, A.V. Nikitin, Methane line parameters in the HITRAN2012 database, J. Quant. Spectrosc. Radiat. Trans. 130 (2014) 201–19. doi:10.1016/j.jqsrt.2013.06.020.
2. O.M. Lyulin, S. Kassi, K. Sung, L.R. Brown, A. Campargue, Determination of the low energy values of $^{13}CH_4$ transitions in the $2\nu_3$ region near 1.66 µm from absorption spectra at 296 and 81 K, J. Mol. Spectrosc. 261 (2010) 91-100. doi:10.1016/j.jms.2010.03.008.
3. A.V. Nikitin, O.M. Lyulin, S.N. Mikhailenko, V.I. Perevalov, N.N. Filippov, I.M. Grigoriev, I. Morino, T. Yokota, R. Kumazawa, T. Watanabe, GOSAT-2009 methane spectral linelist in the 5550-6236 cm^{-1} range, J. Quant. Spectrosc. Radiat. Trans. 111 (2010) 2211-2224. doi:10.1016/j.jqsrt.2014.12.003.
4. A. Campargue, J. Lopez Segovia, S. Béguier, S. Kassi, D. Mondelain, The absorption spectrum of $^{13}CH_4$ in the region of the $2\upsilon_3$ band at 1.66 µm: Empirical line lists and temperature dependence, J. Quant. Spectrosc. Radiat. Trans. 152 (2015) 140-148. doi:10.1016/j.jqsrt.2014.11.012.
5. E. Starikova, A.V. Nikitin, M. Rey, S.A. Tashkun, D. Mondelain, S. Kassi, A. Campargue, Vl.G. Tyuterev, Assignment and modelling of the absorption spectrum of $^{13}CH_4$ at 80 K in the region of the $2\nu_3$ band (5853-6201 cm^{-1}), J. Quant. Spectrosc. Radiat. Trans. 177 (2016) 170–180. doi:10.1016/j.jqsrt.2015.12.023.
6. I.E. Gordon, L.S. Rothman, C. Hill, R.V. Kochanov, Y. Tan, P.F. Bernat, M. Birk, V. Boudon, A. Campargue, K.V. Chance, B.J. Drouin, J.-M. Flaud, R.R. Gamache, J.T. Hodges, D. Jacquemart, V.I. Perevalov, A. Perrin, K.P. Shine, M.-A.H. Smith, J. Tennyson, G.C. Toon, H. Tran, V.G. Tyuterev, A. Barbe, A.G. Császár, V.M. Devi, T. Furtenbacher, J.J. Harrison, J.-M. Hartmann, A. Jolly, T.J. Johnson, T. Karman, I. Kleiner, A.A. Kyuberis, J. Loos, O.M. Lyulin, S.T. Massie, S.N. Mikhailenko, N. Moazzen-Ahmadi, H.S.P. Müller, O.V. Naumenko, A.V. Nikitin, O.L. Polyansky, M. Rey, M. Rotger, S.W. Sharpe, K. Sung, E. Starikova, S.A. Tashkun, J. Vander Auwera, G. Wagner, J. Wilzewski, P. Wcisło, S. Yu, E.J. Zak, The HITRAN2016 molecular spectroscopic database, J. Quant. Spectrosc. Radiat. Trans. 203 (2017) 3-69, doi:10.1016/j.jqsrt.2017.06.038.
7. S. Kassi, B. Gao, D. Romanini, A. Campargue, The near infrared (1.30-1.70 µm) absorption spectrum of methane down to 77 K, Phys. Chem. Chem. Phys. 10 (2008) 4410-19. doi:10.1039/B805947K.
8. M. Rey, A.V. Nikitin, Vl.G. Tyuterev, Predictions for methane spectra from potential energy and dipole moment surfaces: Isotopic shifts and comparative study of $^{13}CH_4$ and $^{12}CH_4$, J. Mol. Spectrosc. 291 (2013) 85–97. doi:10.1016/j.jms.2013.04.003.
9. M. Ghysels, D. Mondelain, S. Kassi, A.V. Nikitin, M. Rey, A. Campargue, The methane absorption spectrum near 1.73 µm (5695–5850 cm^{-1}): Empirical line lists at 80 K and 296 K and rovibrational assignments, J. Quant. Spectrosc. Radiat. Trans. 213 (2018) 169–177, doi:10.1016/j.jqsrt.2018.04.007.
10. M. Rey, A.V. Nikitin, Vl.G. Tyuterev, Theoretical hot methane line lists up to T=2000 K for astrophysical applications, Astrophys. J. 789 (2014) 2. doi:10.1088/0004-637X/789/1/2.
11. M. Rey, A.V. Nikitin, Y. Babikov, Vl.G. Tyuterev, TheoReTS – An information system for theoretical spectra based on variational predictions from molecular potential energy and dipole moment surfaces, J Molec Spectrosc. 327 (2016) 138–158. doi:10.1016/j.jms.2016.04.006.
12. M. Rey, A. V. Nikitin, B. Bézard, A. Coustenis, P. Rannou, V.G. Tyuterev, New accurate theoretical line lists of $^{12}CH_4$ and $^{13}CH_4$ in the 0-13400 cm^{-1} range: application to the modeling of methane absorption in Titan's atmosphere, Icarus 303 (2018) 114-130. doi:10.1016/j.icarus.2017.12.045.
13. S. Kassi, D. Romanini, A. Campargue. Mode by Mode CW-CRDS at 80 K: Application to the 1.58 µm transparency window of CH4. Chem. Phys. Lett. 477 (2009) 7-21. doi:10.1016/j.cplett.2009.06.097.
14. D. Mondelain, S. Kassi, L. Wang, A. Campargue, The 1.28 µm transparency window of methane (7541-7919 cm^{-1}): empirical line list and temperature dependence between 80 K and 296 K, Phys. Chem. Chem. Phys. 17 (2011) 7985-96. doi:10.1039/c0cp02948c.
15. A. Campargue, L. Wang, S. Kassi, D. Mondelain, B. Bézard, E. Lellouch, A. Coustenis, C. de Bergh, M. Hirtzig, P. Drossart, An empirical line list for methane in the 1.26-1.71 µm region for planetary investigations (T= 80-300 K). Application to Titan, Icarus 219 (2012) 110-28. doi:10.1016/j.icarus.2012.02.015.
16. M. Ghysels, S. Vasilchenko, D. Mondelain, S. Béguier S. Kassi, and A. Campargue. Laser absorption spectroscopy of methane at 1000 K near 1.7 µm: A validation test of the spectroscopic databases, J. Quant. Spectrosc. Radiat. Trans. ??? (2018) ??-?? doi:10.1016/j.jqsrt.2018.04.032.
17. A. Campargue, O. Leshchishina, L. Wang, D. Mondelain, S. Kassi, The WKLMC empirical line lists (5852-7919 cm^{-1}) for methane between 80 K and 296 K: "final" lists for atmospheric and planetary applications, J. Mol. Spectrosc. 291 (2013) 16–22. doi:10.1016/j.jms.2013.03.001.

18. A.V. Nikitin, O.M. Lyulin, S.N. Mikhailenko, V.I. Perevalov, N.N. Filippov, I.M. Grigoriev, I. Morino, Y. Yoshida, T. Matsunaga. GOSAT-2014 methane spectral line list, J. Quant. Spectrosc. Radiat. Trans. 154 (2015) 63–71. doi: 10.1016/j.jqsrt.2014.12.003.
19. A.V. Nikitin, M. Rey, V.G. Tyuterev, Accurate line intensities of methane from first-principles calculations, J. Quant. Spectrosc. Radiat. Trans. 200 (2017) 90-99. doi:10.1016/j.jqsrt.2017.05.023.
20. A.V. Nikitin, X. Thomas, L. Régalia, L. Daumont, M. Rey, S.A. Tashkun, Vl.G. Tyuterev, L.R. Brown, Measurements and modeling of long-path $^{12}CH_4$ spectra in the 4800–5300 cm^{-1} region, J. Quant. Spectrosc. Radiat. Trans. 138 (2014) 116–23. doi:10.1016/j.jqsrt.2014.02.005.
21. A.V. Nikitin, X. Thomas, L. Daumont, M. Rey, K. Sung, G.C. Toon, M.A.H. Smith, A.W. Mantz, S.A. Tashkun, Vl.G. Tyuterev, Measurements and modeling of long-path $^{12}CH_4$ spectra in the 5300–5550 cm^{-1} region, J. Quant. Spectrosc. Radiat. Trans. 202 (2017) 255–64. doi:10.1016/j.jqsrt.2017.07.030.
22. A.V. Nikitin, I.S. Chizhmakova, M. Rey, S.A. Tashkun, S. Kassi, D. Mondelain, A. Campargue, Vl. G. Tyuterev. Analysis of the absorption spectrum of $^{12}CH_4$ in the region 5855–6250 cm^{-1} of the $2\nu_3$ band, J. Quant. Spectrosc. Radiat. Trans. 203 (2017) 341–8. doi:10.1016/j.jqsrt.2017.05.014.
23. A. Campargue, L. Wang, D. Mondelain, S.Kassi B. Bézard, E. Lellouch, M. Hirtzig, A Coustenis, C. de Bergh, P. Drossart, Icarus 219 (2012) 110–128.
24. A.V. Nikitin, S. Mikhailenko, I. Morino, T. Yokota, R. Kumazawa, T. Watanabe, Isotopic substitution shifts in methane and vibrational band assignment in the 5560–6200 cm^{-1} region, J. Quant. Spectrosc. Radiat. Trans. 110 (2009) 964–73.

[11] Campargue A, Leshchishina O, Wang L, Mondelain D, S. Kassi, The WKLMC empirical line lists (5852-7919 cm?1) for methane between 80 K and 296 K: "final" lists for atmospheric and planetary applications. J. Molec. Spectrosc. 2013;291: 16-22.
[12] Hirtzig M., Bézard B., Lellouch E., Coustenis A., de Bergh C., Drossart P., Campargue A., Boudon V., Tyuterev V., Rannou P., Cours T., Kassi S., Nikitin A., Mondelain D., Rodriguez S., Le Mouélic S., Titan's surface and atmosphere from Cassini/VIMS data with updated methane opacity. Icarus 2013;226, no. 1: 470-486.
[13] Campargue A., Leshchishina O., Mondelain D., Kassi S., Coustenis A., An improved empirical line list for methane in the region of the 2v3 band at 1.66μm J. Quant. Spectrosc. Radiat. Transfer 2013;118: 49-59.
[14] Nikitin A.V., Thomas X., Regalia L., Daumont L., Von der Heyden P., Tyuterev Vl.G., First assignment of the 5v4 and v2+4v4 band systems of 12CH4 in the 6287-6550 cm-1 region. J. Quant. Spectrosc. Radiat. Transfer 2011;112: 28-40.
[15] Sciamma-O'Brien E, Kassi S, Gao B, Campargue A., Experimental low energy values of CH4 transitions near 1.33 μm by absorption spectroscopy at 81 K. J Quant Spectrosc Radiat Transfer 2009;110:951-63. 2009;110: 951-963.
[16] Wang L, Mondelain D, Kassi S, Campargue A., The absorption spectrum of methane at 80 and 294 K in the Icosad (6717-7589 cm-1): improved empirical line lists, isotopologue identification and temperature dependence. J Quant Spectrosc Radiat. Transfer 2011;113: 47-57.
[17] Campargue A., Wang L., Kassi S., Mašát M., Votava O., Temperature dependence of the absorption spectrum of CH4 by high resolution spectroscopy at 81 K: (II) The Icosad region (1.49-1.30 μm). J Quant Spectrosc Radiat Transfer 2010;1141, no. 51: 111.
[18] Wang L., Kassi S., Liu A.W., Hu S.M., Campargue A., The 1.58γm transparency window of methane (6165-6750cm -1): Empirical line list and temperature dependence between 80 and 296K. J. Quant Spectrosc Radiat Transfer 2011;112: 973-951.
[19] Liu AW., Kassi S., Campargue A., High sensitivity CW-cavity ring down spectroscopy of CH4 in the 1.55 μm transparency window Chem Phys Lett 2007;447: 16-20.
[20] Mondelain D, Kassi S, Wang L, Campargue A., The 1.28 μm transparency window of methane (7541-7919 cm^{-1}): empirical line list and temperature dependence between 80 K and 296 K. Phys Chem Chem Phys 2011;7985-96: 17.
[21] Gao B, Kassi S, Campargue A, Empirical low energy values for methane transitions in the 5852-6181 cm-1 region by absorption spectroscopy at 81 K. J. Molec. Spectrosc. 2009;253: 55-63.